

1

1,2

3

4

:

: 4 cm 가 23

9

14

fast multiplanar spoiled gradient echo

1, 2, 3, 4, 5

가 (peak percentage increase in signal intensity, p%SI)

가

가 (mean percentage increase

in signal intensity, m%SI)

-m%SI

4가

: p%SI  $120.6 \pm 30.7$  (mean  $\pm$  SD)

81.8-171.6

p%SI  $29.5 \pm 21.4$  (mean  $\pm$  SD)

3.7-78.9

p%SI

1

p%SI

(p &lt; 0.0001).

-m%SI

1

가

3

가

가

89%(8/9)

50%(7/14)

50%(7/14)

:

CT

CT

가

Folkman(4) Brem (5)

가

가 (1-3)

2

(6), CT (7-9), (magnetic resonance imaging, MR) (10,11), 2-[fluorine-18]- fluoro-2-deoxy-D-glucose (FDG) PET/SPECT (12-13)

가

(computed tomography, CT) 가

CT

가

가

1  
2  
3  
4

1998

1999 2 1 1999 3 17

(susceptibility artifact)

가



가  
(region of interest)  
(Fig. 1).  
2-4  
3  
가  
CT  
가  
가(percentage increase in  
signal intensity, %SI)  
$$\%SI = (SI_{post} - SI_{pre}) \times 100 / SI_{pre}$$
  
SI<sub>pre</sub> ;  
SI<sub>post</sub> ;  
(peak signal inten-  
sity, pSI)  
가(peak percentage increase in signal intensity, p%SI)  
p%SI  
Wilcoxon rank sum test  
%SI  
(mean percentage increase in signal intensity, m%SI)  
-m%SI

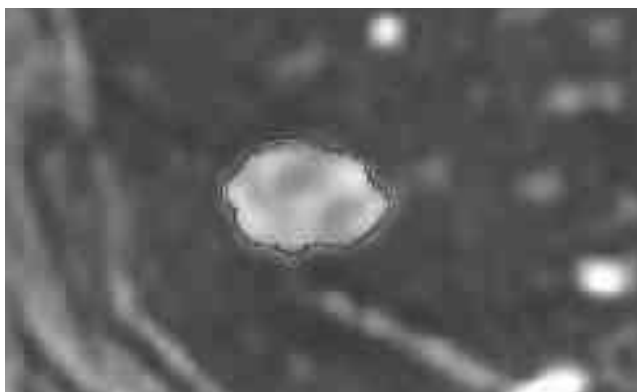


Fig. 1. The measurement of the signal intensity of a solitary pulmonary nodule (SPN). We set the region of interest by a manual drawing along the margin of SPN with care so partial volume effect should be as minimal as possible.

p%SI  
Pearson  
(Table 1).  
4가  
9  
p%SI 120.6 ± 30.7 (mean ± SD)  
81.8 171.6 14  
p%SI 29.5 ± 21.4 (mean ± SD)  
3.7 78.9 (Table 1). p%SI  
1  
가 (p<0.0001 by Wilcoxon rank sum  
test) (Fig. 2). p%SI (cut-off value) 80  
가 100%  
9 8 (89%) 3 p%SI  
14 10 (71%) 3  
p%SI (Table 1). m%SI 1  
가  
3 가 가 (plateau)  
(Fig. 3).  
27.9mm, 17-37mm  
24.5mm, 17-40mm  
p%SI  
p%SI (r = -0.84)  
(r = -0.17).  
9 8 (89%)  
(Fig. 4) 1 (11%)  
14 7 (50%)

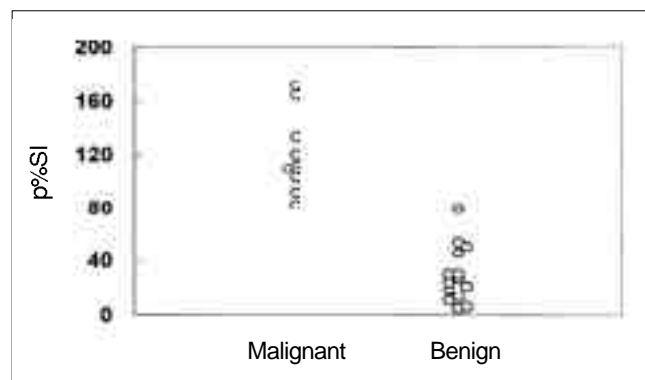


Fig. 2. The peak percentage increase in signal intensity (p%SI) of malignant and benign solitary pulmonary nodules (SPNs). With the cut-off value of 80 p%SI, graph shows no overlap of the p%SI between malignant and benign SPNs.

(Fig. 5), 7 (50%)  
 ( , , , ), ,  
 , CT (1-3). 1990  
 Littleton (6)

CT MR  
 가 (14,15)

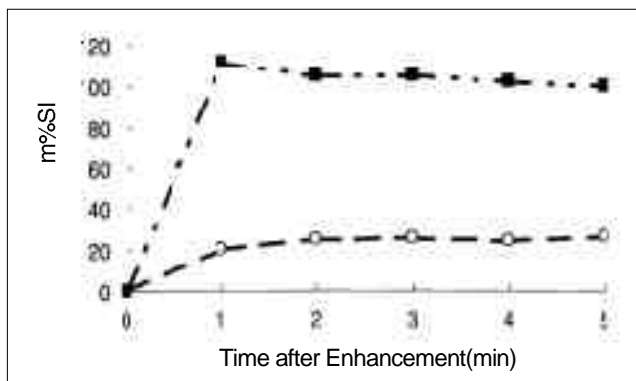


Fig. 3. The time-m%SI (mean percentage increase in signal intensity) curve. The m%SI of malignant SPNs rapidly increased at 1 minute and decreased gradually thereafter, whereas that of benign SPNs more slowly increased to form a plateau.

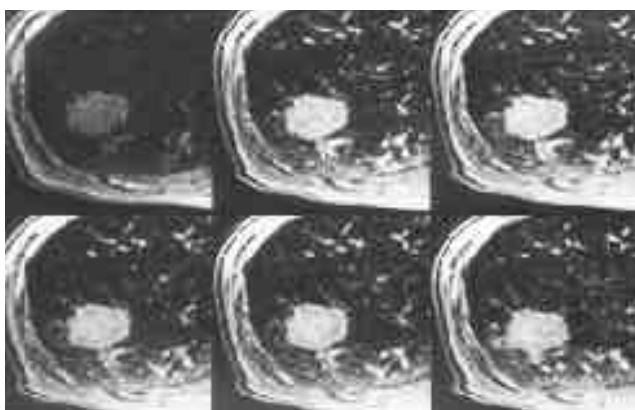


Fig. 4. 73-year-old man with small cell carcinoma (patient 8). Serial MR images show homogeneous enhancement of SPN. The p%SI is reached in 2 minutes after contrast enhancement (Top right).

가 (14,15).

가

(16).

p%SI (cut-off value) 80 (Fig. 2).

(Table 2). FMPSPGR  
 (gradient echo signal) (spin echo signal)

(17).

(Static)

T1 Kono (11)  
 Guckel (10)  
 Kono (11) 0.1mmol/kg 1  
 Guckel (10) 0.05mmol/kg  
 (4 ) (bolus injection)

가  
 가  
 가  
 12 cc ( 60kg ,  
 0.1mmol/kg 1

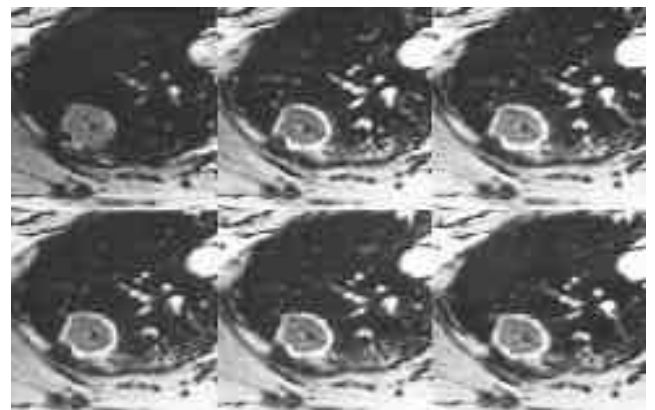


Fig. 5. 39-year-old man with tuberculoma (patient 18). Serial MR images show peripheral rim-like enhancement of SPN. The nodule has small cavity in the center. The p%SI is reached in 2 minutes (Top right) and forms a plateau thereafter.

**Table 2. Summary of Reported Results of Enhancement Characteristics between Malignant and Benign Solitary Pulmonary Nodules (SPNs)**

	Modality	Malignant	Benign	Parameter	P value
Kono et al (11)	T1-weighted SE (D)	62	23	%SI	< 0.001
Gückel et al (10)	T1-weighted SE (S)	53.4 *	33.0 *	%SI	> 0.2
Gückel et al (10)	Snapshot GRE (D)	18.1 *	2.3 *	%SI/sec	< 0.0001

SE= spin echo, D= dynamic MRI, S= static MRI, GRE= gradient echo

FMPSPGR= fast multiplanar spoiled gradient echo

\* = median value      = mean value

%SI= percentage increase in signal intensity

**%SI/sec= percentage mean slope of time-intensity curve of nodule**

$$= (\text{SI}_{\text{postcontrast}} - \text{SI}_{\text{precontrast}}) \times 100 / \text{SI}_{\text{precontrast}} \times (\text{T}_{\text{max-art}} - \text{T}_{0\text{-art}})$$

where, T<sub>max-art</sub>= time of maximal SI of pulmonary artery during the first transit of the bolus of contrast material

$T_0$ -art= time before the arrival of the bolus of contrast material in the pulmonary artery

(reproducibility)

p%SI

CT

가

(partial volume effect)

Yamashita (9)

60%

Swensen (7)

Gückel (10)

가

1-2mm

가가

specimen

3

가

Fumikazu (19)

가

88%(7/8)

(Fig. 1).

Yamashita (9)

Swensen (7)

p%SI

(pitfall)

5).

(Fig. 4).

89% (8/9)

5

p%SI

Kono (11)

T1

Fumikazu (20)

가

가

가

(20).

Swensen (8)

m%SI

(Fig. 3)

Gückel (10)

Gückel (10)

(first pass)

가

(slope, %SI/sec)

가

(Table 2).

(peak)

(interstitial space)

(18).

(18)

Murayama(21)

CT

12

3

가

2

가

(22).

가

가 5 . Gurney(1)  
1% 2 가 (doubling time)  
가 Yankelevitz (23)

2  
가  
가  
가  
1  
가

1. Gurney JW. Determining the likelihood of malignancy in solitary pulmonary nodules with Bayesian analysis. I. Theory. *Radiology* 1993;186:405-413
2. Shulkin AN. Management of the indeterminate solitary pulmonary nodule: a pulmonologist's view. *Ann Thorac Surg* 1993;56:743-744
3. Siegelman SS, Khouiri NF, Leo FP, Fishman EK, Braverman RM, Zerhouni EA. Solitary pulmonary nodules: CT assessment. *Radiology* 1986;160:307-312
4. Folkman J. Tumor angiogenesis: therapeutic implications. *N Engl J Med* 1971;285:1182-1186
5. Brem S, Cotran R, Folkman J. Tumor angiogenesis: a quantitative method for histologic grading. *J Natl Cancer Inst* 1972;48:347-356
6. Littleton JT, Durizch ML, Moeller G, Herbert DE. Pulmonary masses: contrast enhancement. *Radiology* 1990;177:861-871
7. Swensen SJ, Brown LR, Colby TV, Weaver AL, Midthun DE. Lung nodules enhancement at CT: prospective findings. *Radiology* 1996;201:447-455
8. Swensen SJ, Brown LR, Colby TV, Weaver AL. Pulmonary nodules: CT evaluation of enhancement with iodinated contrast material. *Radiology* 1995;194:393-398

9. Yamashita K, Matsunobe S, Tsuda T, Nemoto T, Matsumoto K, Miki H, Konishi J. Solitary pulmonary nodule: preliminary study of evaluation with incremental dynamic CT. *Radiology* 1995;194:399-405
10. Gückel C, Schnabel K, Deimling M, Steinbrich W. Solitary pulmonary nodules: MR evaluation of enhancement patterns with contrast-enhanced snapshot gradient-echo imaging. *Radiology* 1996;200:681-686
11. Kono M, Adachi S, Kusumoto M, Sakai E. Clinical utility of Gd-DTPA-enhanced magnetic resonance imaging in lung cancer. *J Thorac Imaging* 1993;8(1):18-26
12. Worsley DF, Cellar A, Adam MJ et al. Pulmonary nodules: differential diagnosis using 18F-fluorodeoxyglucose single-photon emission computed tomography. *AJR* 1997;168:771-774
13. Gupta NC, Maloof J, Gunel E. Probability of malignancy in solitary pulmonary nodules using fluorine-18-FDG and PET. *J Nucl Med* 1996;37:943-948
14. Buadu LD, Murakami J, Murayama S, et al. Breast lesions: correlation of contrast medium enhancement patterns on MR images with histopathologic findings and tumor angiogenesis. *Radiology* 1996;200:639-649
15. Frouge C, Guinebretiere J-M, Contesso G, DiPaola R, Blery M. Correlation between contrast enhancement in dynamic magnetic resonance imaging of the breast and tumor angiogenesis. *Invest Radiol* 1994;29:1043-1049
16. Passe TJ, Bleumke DA, Siegelman SS. Tumor angiogenesis: tutorial on implications for imaging. *Radiology* 1997;203:593-600
17. 1998: 169-189
18. Griebble J, Nayr NA, Alexander de V et al. Assessment of tumor microcirculation: a new role of dynamic contrast MR imaging. *J Magn Reson Imaging* 1997;7:111-119
19. Sakai F, Sone S, Maruyama A et al. Thin-rim enhancement in Gd-DTPA-enhanced magnetic resonance images of tuberculoma: a new finding of potential differential diagnostic importance. *J Thorac Imaging* 1992;7(4):64-69
20. Sakai F, Sone S, Kiyono K et al. MR of pulmonary hamartoma: pathologic correlation. *J Thorac Imaging* 1994;9:51-55
21. Murayama S, Murkami J, Hashimoto S, Torii Y, Masuda K et al. Noncalcified pulmonary tuberculomas: CT enhancement patterns with histological correlation. *J Thorac Imaging* 1995;10:91-95
22. Hittmair K, Eckersberger F, Klepetko W, Helbich T, Herold CJ. Evaluation of solitary pulmonary nodules with dynamic contrast-enhanced MR imaging- a promising technique? *Magn Reson Imaging* 1995;7:923-933
23. Yankelevitz DF, Henschke CI. Does 2-year stability imply that pulmonary nodules are benign? *AJR* 1997;168:325-328

## Differentiation of Benign and Malignant Solitary Pulmonary Nodules : Value of Contrast-Enhanced Dynamic MR Imaging<sup>1</sup>

Jeong-Ho Kim, M.D., Hyung-Jin Kim, M.D., Heon Han, M.D.<sup>1,2</sup>, Hong Lyeol Lee, M.D.<sup>3</sup>, Kwang Ho Kim, M.D.<sup>4</sup>, Chang Hae Suh, M.D.

<sup>1</sup>Department of Radiology, Inha University, College of Medicine, Incheon, Korea

<sup>2</sup>Department of Radiology, Kangwon University College of Medicine

<sup>3</sup>Department of Internal Medicine, Inha University, College of Medicine, Incheon, Korea

<sup>4</sup>Department of Thoracic and Cardiovascular Surgery, Inha University, College of Medicine, Incheon, Korea

**Purpose :** To evaluate the usefulness of contrast-enhanced dynamic MR imaging for differentiation of benign and malignant solitary pulmonary nodules (SPNs).

**Materials and Methods :** Twenty-three patients with histologically or radiologically proven SPNs smaller than 40mm (14 benign, 9 malignant) underwent MR examination using the breath-hold fast multiplanar spoiled gradient echo (FMPSPGR) technique. Pre-enhancement MR examination was followed by serial scans obtained at one-minute intervals, beginning one-minute after the onset of bolus injection of paramagnetic contrast agent for a total of five scans. Signal intensities of SPNs were measured from pre- and post-contrast enhanced MR images and peak percentage increase in signal intensity (p%SI) was calculated. Mean percentage increase in signal intensity (m%SI) was also calculated and the time-m%SI curve was plotted. The enhancement patterns of SPNs were classified as homogeneous, peripheral rim-like, inhomogeneous, or no (or minimal) enhancement. We compared differences in p%SI, the pattern of the time-m%SI curve, and the pattern of enhancement between benign and malignant SPNs.

**Results :** On dynamic MR images, malignant SPNs (n= 9) showed a significantly higher p%SI than benign SPNs (n= 14) (malignant : mean 120.6, range 81.8-171.6; benign: mean 29.5, range 3.7-78.9) ( $p < 0.0001$ ). With 80 p%SI as the threshold for malignancy-positive, both sensitivity and specificity were 100%. The m%SI of malignant SPNs rapidly increased at one minute after enhancement and decreased gradually thereafter, whereas that of benign SPNs increased more slowly to form a plateau. Eighty-nine percent (8/9) of malignant SPNs showed homogeneous enhancement. In contrast, among benign SPNs, peripheral rim-like enhancement and no (or minimal) enhancement occurred in the same proportion of cases : 50% (7/14).

**Conclusion :** The superb demonstration of different enhancement characteristics obtained using dynamic contrast-enhanced MR imaging is useful to discriminate malignant from benign SPNs.

**Index words :** Lung neoplasms, diagnosis  
Lung neoplasms, MR  
Lung, nodule

Address reprint requests to : Hyung-Jin Kim, M.D., Department of Radiology, Inha University Hospital,  
#7-206 3rd St., Shinheung-dong, Choong-ku, Incheon, 400-103, Korea.  
Tel. 82-32-890-2769 Fax. 82-32-890-2743